RSC Applied Polymers

ROYAL SOCIETY OF CHEMISTRY

PAPER

View Article Online
View Journal | View Issue

Cite this: *RSC Appl. Polym.*, 2026, **4**, 767

Fabrication of gallic acid crosslinked chitosan/poly(1-vinylpyrrolidone-*co*-vinyl acetate) antioxidant films for green chilli packaging

Bhagyalakshmi A. Sheeparamatti,[a] Priyanka Baburao,[a] Priyadarshini,[a] Shiddalingesh G. Havanur,[a] Ravindra B. Chougale,*[a] Manjushree Nagaraj Gunaki,[b] Ajitkumar Appayya Hunashyal,[b] Saraswati P. Masti,[b] Nagarjuna Prakash Dalbanjan[c] and S. K. Praveen Kumar[c]

In this study, chitosan (CS)/poly(1-vinylpyrrolidone-*co*-vinyl acetate) (PVP-*co*-VAc) films were fabricated by incorporating different weight fractions of gallic acid (GA), abbreviated as CPG, using the solvent casting method. The prepared films were investigated for their physicochemical properties. Fourier transform infrared spectroscopy (FTIR), X-ray diffraction (XRD) and scanning electron microscopy (SEM) micrographs revealed the effective interaction between the added GA and the CS/poly(1-vinylpyrrolidone-*co*-vinyl acetate) polymer matrix. The resultant films demonstrated good barrier properties against water and oxygen, which were further supported by water contact angle (WCA) findings. Also, the films exhibited excellent mechanical properties with a tensile strength (TS) of 54.71 ± 0.62 MPa, which is more substantial than those of traditional polythene plastics (10–16 MPa). Compared with the CP film, the CPG-IV film with the highest weight percentage of GA exhibited a strong DPPH radical scavenging activity of 77.18% ± 0.020 and displayed vigorous antimicrobial activity against *Staphylococcus aureus*, *Escherichia coli*, and *Candida albicans*. Also, the packaging study revealed that chillies packed with the CPG-IV film containing the highest amount of GA showed a limited weight loss percentage in comparison with unpacked chillies and those packed with a polyethylene film over 14 days of storage. The above results suggested that the prepared films meet the essential requirements of green chilli packaging applications.

Received 29th October 2025,
Accepted 13th January 2026

DOI: 10.1039/d5lp00339c

rsc.li/rscapplpolym

1. Introduction

In the current scenario, packaging and preservation of food are more prominent in the food industry to prevent food from microbial contamination.[1] To meet consumer demands, packaging industries are taking extreme care to ensure food safety. Innovative polymeric materials have revolutionized the food packaging sector in the last decade.[2] Recently, synthetic polymers manufactured from nonrenewable petroleum resources like polyethene, polypropylene, polyester, polyvinyl alcohol, and polyamide have been used to prepare packaging materials in the food sector due to their strength, flexibility, ease of production, and excellent barrier properties.[3] Plastic manufacturing has surged from roughly 8 billion tons during World War II to around 235 billion tons today, with production expected to double further by 2035.[4] These plastic materials are ultimately responsible for environmental pollution and may also enter the food chain, causing serious health problems for animals and human beings.[5] Thus, depletion of fossil fuels leads to further use of renewable resources, such as products derived from plants and animals, in the development of packaging materials.[6] As a result, a lot of research is being done to produce environmentally friendly materials. Thus, biopolymers play a prominent role in sustaining future generations by developing packaging materials using products and by-products derived from agricultural fields and biological waste.[7]

Biodegradable polymers, which include synthetic and natural polymers, serve as alternatives to petroleum-based plastics. When they are exposed to the environment, they will form nontoxic constituents such as water and carbon dioxide.[8] Biodegradable polymers in packaging reduce plastic pollution and reliance on fossil fuels. Also, they maintain the food's freshness by acting as barriers to water and oxygen. Among all the biodegradable polymers, chitosan (CS) plays a major role in packaging applications in addition to its biodegradability, film-forming quality, and chelating property. CS is a derivative

[a]*PG Department of Studies in Chemistry, Karnatak University, Dharwad, 580 003 Karnataka, India. E-mail: chougaleravindra@yahoo.com, ravindraabc@kud.ac.in*
[b]*Department of Chemistry, Karnatak Science College, Dharwad, 580 001 Karnataka, India*
[c]*PG Department of Studies in Biochemistry, Karnatak University, Dharwad 580003, Karnataka, India*

of chitin; the potential polymer chitosan has drawn a lot of attention from the packaging sector.[9,10] Also, it is the second largest polymer obtained from nature, next to cellulose.[11] The protonation of NH_2 groups of the chitosan backbone allows it to dissolve in low-pH solutions like acetic acid, which is responsible for microbial inhibition.[12,13] Despite these advantages, it has some drawbacks, like brittleness, hydrophilicity, and poor mechanical properties. To enhance CS properties, it is combined with polymers like PLA, PVA, and (PVP-*co*-VAc).[14–16] Hence, using (PVP-*co*-VAc) in the blend can induce a plasticizing effect, thereby reducing the brittleness of the film.

Poly(1-vinylpyrrolidone-*co*-vinyl acetate) (PVP-*co*-VAc) is a synthetic biodegradable polymer suitable for food packaging, and it is obtained by the polymerization of vinylpyrrolidone with vinyl acetate.[17] Indeed, the combined use of (PVP-*co*-VAc) and CS can create a polymer network through intermolecular hydrogen bonding, resulting in better mechanical and functional properties. (PVP-*co*-VAc) has importance in the pharmaceutical industry and cosmetic industry because of its adhesive qualities and affinity towards various substances and surfaces. (PVP-*co*-VAc) is soluble in water and can be easily eliminated through metabolic pathways.[18] The film-forming property of (PVP-*co*-VAc) enables it to combine with polymers to form packaging films in the food packaging industry.

Active packaging accounts for the introduction of active moieties to attain the required functionalities, mainly to preserve food, while intelligent packaging mainly focuses on signaling the visual quality of food to prolong its shelf life.[4] Active agents keep the food fresh and minimize food spoilage by preventing the interaction of water and oxygen with it. Nowadays, food packaging materials that incorporate active ingredients such as antioxidants and antibacterial agents, as well as active and intelligent packaging techniques, are becoming increasingly important since they increase human safety.

Gallic acid (GA) is a natural polyphenolic compound present in grapes, several berries, and green tea.[19] It is characterized by three hydroxyl groups that enable strong hydrogen bonding interactions, and the presence of a benzene structure in the gallic acid provides mechanical support, which helps in preventing physical impacts from external factors on food packaging films[20] and in preventing food deterioration. Additionally, a survey conducted by the U.S. FDA found that GA is a safe compound. Numerous pharmacological actions, including antibacterial, antiviral, and anti-inflammatory effects, have been demonstrated by gallic acid.[21]

Some researchers have studied the effect of GA on biodegradable polymeric films. GA-incorporated PT blend films showed good tensile strength (TS) and elongation at break (EB) values, as reported by Goudar N *et al.*[22] It was found that the shelf life of grapes coated with a GPP (GA, PVA and phycocyanin) hydrogel was noticeably extended up to 13 days.[23] Additionally, photodynamically-mediated chitosan–nanocellulose-based films crosslinked with GA extended the shelf life of oysters by reducing lipid oxidation.[24] Raja Venkatesan *et al.* (2024) developed PBAT/CL films crosslinked with varying weight percentages of GA, which showed good antibacterial properties and contributed to the increased shelf life of strawberries.[25] GA-incorporated CS/PUL films showed good mechanical and UV barrier properties as demonstrated by Min Zhang *et al.*[26] Recent studies suggested that GA-incorporated films were eventually developed as sustainable, eco-friendly packaging materials. These packaging materials were tested for packaging efficiency using green chillies as a packaged material. The goal of the current work is to develop CS/(PVP-*co*-VAc) films crosslinked with various GA weight fractions, and the most perishable vegetable, green chillies, was selected for this study. The resultant properties were compared with those of CS-based and CS/(PVP-*co*-VAc) blend-based films. According to the literature review, CS/(PVP-*co*-VAc) films with GA have not yet been published. Furthermore, the goal of this work is to assess the efficiency of CPG films towards storage and prolonging the shelf life of green chillies at room temperature.

2. Materials and methods

2.1. Materials

Chitosan (CS) flakes (20–100 kDa; degree of deacetylation of 75–85%) having a viscosity of 200 cps were sourced from Loba Chemie Pvt Ltd, Mumbai. The poly(1-vinylpyrrolidone-*co*-vinyl acetate) copolymer formed by the combination of vinylpyrrolidone and vinyl acetate in the ratio 7 : 3 with 50% ethanol was provided by Tokyo Chemical Industry Co., Ltd. (TCI), Japan. Gallic acid (GA) was purchased from Loba Chemie Pvt Ltd, Mumbai. Acetic acid and ethanol were obtained from Merck Life Science Pvt Ltd, Mumbai. Experiments were done using double distilled water.

2.2. Fabrication of films

The solvent casting method was used to prepare the films. Initially, 2% acetic acid was used to dissolve 1.2 g of CS, and unwanted particles were filtered out from the solution. Conversely, 1 g of poly(1-vinylpyrrolidone-*co*-vinyl acetate) was dissolved in double distilled water to make a 1% solution. Then, various weight fractions of gallic acid were dissolved in 10 mL of 1 : 1 ethanol. Chitosan and (PVP-*co*-VAc) solutions were agitated for 24 h, and various weight fractions of gallic acid were added to the blend and stirred for about 4 h. The resulting solutions were poured onto a dried Petri plate and allowed to dry for 48 h at 35 °C. The films were separated from the Petri plates and were named CP, CPG-I, CPG-II, CPG-III, and CPG-IV based on the gallic acid content in the film. Further analysis was carried out by placing films in a desiccator containing anhydrous $CaCl_2$ (Table 1).

Table 1 Compositions of the prepared biofilms

Sample code	CS (g)	PVP-*co*-VAc (g)	Gallic acid (wt%)
CP	1.2	1	—
CPG-I	1.2	1	1%
CPG-II	1.2	1	2%
CPG-III	1.2	1	3%
CPG-IV	1.2	1	4%

2.3. Fourier transform infrared (FTIR) spectroscopy

The molecular interactions of the fabricated films were studied with the help of an attenuated total reflectance–FT-IR (ATR-FTIR) spectrometer. In brief, films of size 2 × 2 cm^2 were analyzed using the ATR-FTIR spectrometer (Bruker 2 Alpha) at room temperature with 4 cm^{-1} resolution over the IR range of 4000–400 cm^{-1}.

2.4. Scanning electron microscopy (SEM)

The surface morphology of the films was studied by using a scanning electron microscope (JEOL, JSM-IT500LA) with a magnification of 5 μm. A surface study was done in accordance with the ASTM F1372 standard, where the prepared films with a size of 2 × 2 cm^2 were coated with a gold layer before analysis and adhered on a metal stub using double-sided carbon sticky tape at an acceleration voltage of 10 kV.

2.5. Atomic force microscopy (AFM)

Atomic microscopy was used to study the surface morphology of films with the help of a Nanosurf Easyscan 2 microscope (Switzerland) with an aluminum-coated cantilever. The surface roughness was analyzed qualitatively by capturing images at different locations.

2.6. X-ray diffraction (XRD)

An X-ray diffractometer (Rigaku SmartLab, Japan) was used to study the structural properties of the prepared films. Each film sample (2.5 × 2.5 cm^2) was set up on a sample holder. Every film was scanned between an angle range of 2θ = 5°–80° with a speed of 5° min^{-1}. The crystallinity was calculated in terms of percentage using eqn (1).

$$\%\ \text{of crystallinity} = \frac{\text{total area of crystalline peaks}}{\text{total area of all peaks}} \times 100 \quad (1)$$

2.7. Thickness and mechanical properties

A digital micrometer (Mitutoyo, Japan) was used to analyze the thickness of films by taking measurements at three distinct positions with 0.001 mm precision.

Flexibility and stress-withstanding capacity were important parameters of the film. Mechanical properties were investigated with the help of a DAK System Inc. Universal Testing Machine (Series 7200-1 KN) at room temperature in accordance with the ASTM-D882 standard. Samples with a size of 2.5 × 10 cm^2 were placed in the extension grip having a separation of 50 mm, and films were stretched at a rate of 1 mm per minute. Three readings were taken and they were averaged.

2.8. Water contact angle (WCA)

The surface wettability nature of the film was studied using a sessile drop WCA machine DMs-401 model, made in Kyowa Interface Science Co. Ltd using the ASTM D-5946 method. A water droplet was mounted on the surface of the film placed on the sample holder. Then, an image between the film surface and the water droplet was captured using a camera. Three different readings were taken at different places on the surface of the film, and then all were averaged. The results were averaged by taking three readings separately during analysis.

2.9. Optical parameters

Optical properties were investigated using a LAMBDA 365 (PerkinElmer, USA) UV spectrophotometer. The film samples (3 × 1 cm^2) were kept inside a UV cell. The spectral analysis was conducted in the wavelength range of 200–800 nm in accordance with the standard ASTM D4329 method. Transparency and opacity were calculated according to the previously reported literature by Kurabetta *et al.* at a wavelength of 600 nm using eqn (2) and (3).[27]

$$T_{600} = \frac{-\log(\%T)_{600}}{t} \quad (2)$$

$$\text{Opacity} = \frac{A_{600}}{t} \quad (3)$$

where $\%T_{600}$ is the percentage transmittance at 600 nm, A_{600} is the absorbance and t is the thickness of the film.

2.10. Hydration properties

The films of size 2 × 2 cm^2 were dried in an oven for 24 h at 50 °C to measure water absorption capacity in accordance with the ASTM standard D570-98 guidelines. The weight of the films was measured and recorded as the initial weight (W_0). Then films were dipped into a beaker containing 20 mL of double distilled water. Again, they were weighed after 12 h; before weighing, these films were blotted with filter paper. The weight was measured after absorption of water (W_t). The water absorption ability of gallic acid crosslinked films was calculated with eqn (4).

$$\%\ \text{of water absorption} = \frac{W_t - W_0}{W_t} \times 100 \quad (4)$$

In accordance with the ASTM standard D570-98 method, the films were further dried at 50 °C for 24 h. Then the films were cooled to room temperature and reweighed; this weight was recorded as the dry weight following water absorption (W_d). The water solubility of the films was calculated using eqn (5).

$$\%\ \text{of water solubility} = \frac{W_0 - W_d}{W_0} \times 100 \quad (5)$$

2.11. Barrier properties

Water vapor transmission rate (WVTR). The WVTR test was performed in accordance with the ASTM standard 1249, according to the results obtained by Gasti *et al.*[28] Using Teflon tape, the prepared films were wrapped around the mouth of glass vials containing 10 ml of double distilled water. The initial weight was recorded as W_i. The vials were placed in the oven at 40 °C for 24 h. The glass vials were measured after

being taken out of the oven after 24 h, and the weight was recorded as W_f. Using eqn (6), the WVTR was calculated:

$$\text{WVTR} = \frac{W_i - W_f}{A} \times T \quad (6)$$

where A is the area of cross section of the vial and T is the time duration (24 h).

Oxygen permeability (OP). The OP test was carried out according to the ASTM standard 1307 to determine the oxygen permeability through gallic acid crosslinked films. The mouth of the glass vials was wrapped using films with Teflon tape. The initial weight of the vials was recorded as W_i. The vials were then placed in a desiccator and again the weight was taken for three sequential days, every 24 h. Using eqn (7), the oxygen permeability transmission rate (OPTR) was calculated:

$$\text{OPTR} = \frac{\text{slope}}{\text{film area}} \quad (7)$$

A linear regression curve was used to find the slope of the weight change *vs*. time curve.

The oxygen permeability (OP) was analyzed using eqn (8).

$$\text{OP} = \frac{\text{OPTR} \times L}{\Delta P} \quad (8)$$

Here, L is the average film thickness and ΔP is the variation in the partial pressure between water and the dry atmosphere (0.02308 at 25 °C).

2.12. Differential scanning calorimetry (DSC)

The thermal stability of the prepared films was predicted with a DSC instrument model SET-DSC/SA (SETLINE DSC/SA France/Switzerland) using Calisto software. The film samples were heated from room temperature to 500 °C under an inert N_2 atmosphere in an aluminium crucible.

2.13. Titration of free amine groups

The free amine content of the film was calculated by using the acid–base back titration method. The films were cut into small pieces and dried in an oven at 40 °C for 24 h. 0.01 M (M_1) HCl (25 mL) was poured into a beaker containing 1 g (W) of film sample to protonate the available amine groups. This mixture was continuously stirred for about 24 h to ensure interaction between the acid and amine groups. Under similar conditions, a blank solution was prepared without a film. Then solutions with films and without films were titrated against a 0.01 M NaOH (M_2) solution using a phenolphthalein indicator until a pale pink endpoint was observed. The free amine content provides the quantitative measure of the extent of amine groups involved in crosslinking and was calculated using eqn (9). Also, the reduction of free amine content on addition of the crosslinking agent is given by eqn (10).

$$\text{Free amine} = \frac{(V_1 - V_2) \times M_2}{W} \quad (9)$$

where V_1 is the volume of the NaOH solution for the blank and V_2 is the volume of NaOH for the sample.

$$\text{Reduction of free amine} = \frac{A_1 - A_2}{A_1} \times 100 \quad (10)$$

where A_1 is the free amine content of the control CP film and A_2 is the free amine content of the GA crosslinked films.

2.14. Overall migration test

The overall migration study was carried out according to the ASTM standard 9845. In this method, film samples were measured, and the weight was recorded as W_i; then the samples were dipped into a beaker containing food stimulants, *viz*, distilled water, 50% ethanol, and 3% acetic acid, and kept in an oven at 40 °C for 10 days. After 10 days, the weight was further recorded as W_f. The effect of the food stimulants on food items was calculated using the gravimetric method, and the amount of extract was determined using eqn (11).

$$\text{Amount of extract (\%)} = \frac{W_i - W_f}{S} \quad (11)$$

where S is the area of the film taken.

2.15. Antimicrobial properties

In Mueller–Hinton Agar (MHA) medium, according to the well diffusion method, the antibacterial characteristics of gallic acid crosslinked films were tested against *E. coli* (ATCC 10799) and *S. aureus* (ATCC 6538) bacteria and *C. albicans* (ATCC 24433). Bacterial medium was subcultured employing Luria broth, where the optical density was kept at 0.5 at 600 nm. Using a swab, the microbes were dispersed over a 4 mm thick MHA medium. By considering distilled water as a solvent control, previously made wells of 8 mm diameter were filled with 100 mL of sample solution. Bacterial and microbial developments were observed overnight at 37 °C. Using a Vernier scale, inhibitory zone measurements were taken sequentially.

2.16. Antioxidant properties

The radical scavenging activity of CPG films was determined using DPPH (2,2-diphenyl-1-picrylhydrazyl), methanol, and standard ascorbic acid (1 mg ml^{-1}). Analysis was carried out by dissolving the films and the volume was made up to 1000 μL. The samples were made to react with 100–500 μL of DPPH (0.5 mM) and incubated for 30 min at room temperature. A 1.5 ml glass cuvette having a pathlength of 1 cm was placed in a UV–visible spectrophotometer (Labman, LMSP UV-1200), then the absorbance was measured at 517 nm. Pure methanol was used as a blank solution, while methanol diluted with DPPH solution was considered as a control. The results were expressed as a percentage of inhibition according to eqn (12).

$$\text{\% scavenging} = \frac{\text{Ab}_c - \text{Ab}_s}{\text{Ab}_c} \times 100 \quad (12)$$

2.17. Packaging studies

The fabricated gallic acid combined chitosan/(PVP-*co*-VAc) films were tested for the preservation studies for extending the

storage life of green chillies. A packaging study was carried out by considering unpacked chillies as a reference. A pouch of size 6 × 6 cm^2 was made by using the prepared films and from a polyethylene bag, and packing of chillies was done at room temperature. Every two sequential days, the physical texture was captured using a camera. Furthermore, the weight loss percentage was determined using eqn (13).

$$\% \text{ of weight loss} = \frac{W_i - W_f}{W_i} \times 100 \quad (13)$$

W_i is the initial weight of chillies and W_f is the final weight of chillies.

After packaging, 1 g of each chilli sample was agitated in a rotary shaker at 150 rpm. Then, the obtained solution was spread out on agar plates and incubated for 24 h at 38 °C. Then, using OpenCFU colony software, the colonies were counted. Using eqn (14), the CFUs per gram of chillies were calculated using the following equation:

$$\text{CFU g}^{-1} = \frac{(\text{number of colonies} \times \text{dilution factor} \times 10)}{(\text{volume plated in } \mu\text{l})} \quad (14)$$

2.18. Statistical analysis

OriginPro software was employed to carry out statistical analysis. Using Tukey's test ($p < 0.05$) in the one-way ANOVA program, the triplicate results were taken. The standard deviation method was used for further calculations.

3. Results and discussion

3.1. Fourier transform infrared (FTIR) spectroscopy

The possible interactions between the different functional groups in the CS/(PVP-*co*-VAc)/GA matrix were studied with the help of an FTIR spectroscopic method (Fig. 1). The FTIR spectra of the GA-incorporated films are displayed in Fig. 2. The –NH and –OH stretching vibrations were observed for the distinct broad peak at 3270 cm^{-1} in the CP film. The –CH stretching is confirmed by the appearance of a peak at 2970 cm^{-1}, which is due to the $-CH_2$ group; the band at 1652 cm^{-1} is accounted for by the acetyl group (amide-I) due to C═O stretching. Also, –NH stretching and bending vibration (amide-II) appears for the band at 1542 cm^{-1}. The peaks obtained at 3350 cm^{-1} and 2920 cm^{-1} were responsible for alcoholic –OH stretching and asymmetric –CH (pyrrole ring) in (PVP-*co*-VAc), respectively.

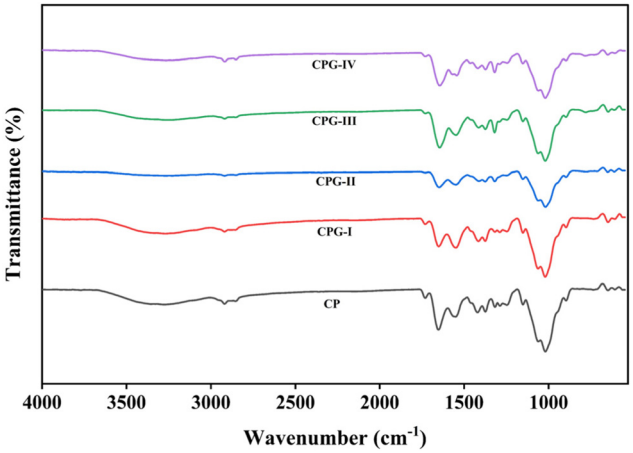

Fig. 2 FTIR spectra of GA crosslinked CS/(PVP-*co*-VAc) films.

The peaks recorded at 1217 cm^{-1} and 1022 cm^{-1} correspond to ester moieties in (PVP-*co*-VAc) for PVAc. The spectra of GA-added films showed negligible differences in comparison with the CP film. The GA-incorporated CPG-I, CPG-II, CPG-III, and CPG-IV films exhibited the –OH stretching frequency peak, which was shifted towards 3330 cm^{-1} from 3270 cm^{-1}, indicating an increase in intermolecular hydrogen bonding, and showed increased tensile strength in the film.[29] Likewise, in GA crosslinked films, the bands at 1652 cm^{-1} and 1542 cm^{-1} moved to lower wavenumbers 1648 cm^{-1} and

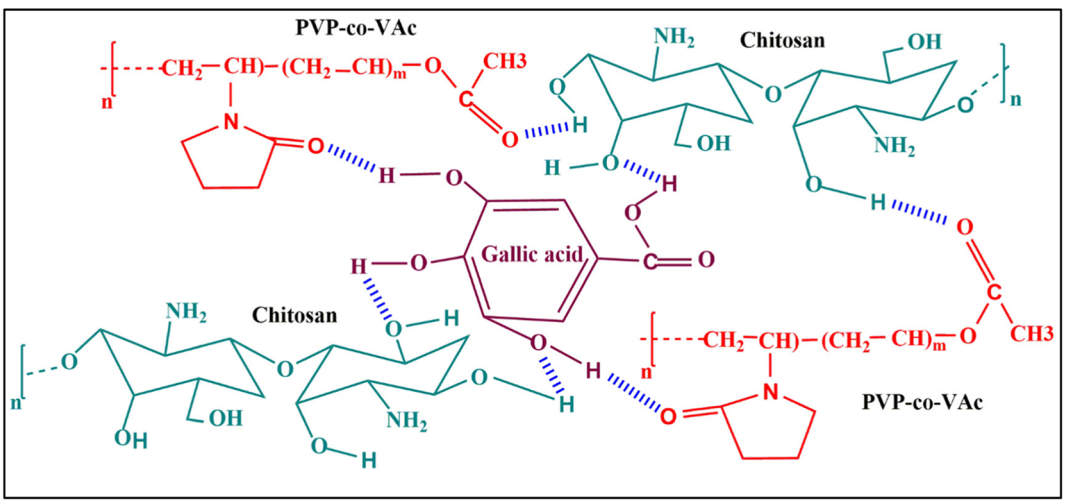

Fig. 1 Plausible intermolecular interactions between different functional groups in the CS/(PVP-*co*-VAc)/GA films.

1540 cm^{-1}, respectively, in GA-incorporated films. This shift was due to the strong bonding interaction between hydroxyl groups of CS/(PVP-*co*-VAc)/GA.

3.2. Scanning electron microscopy (SEM)

Fig. 3 displays the surface morphologies of CP, CPG-I, CPG-II, CPG-III, and CPG-IV films. The CP film had a smooth, homogeneous surface devoid of cracks and fractures. The surface morphology of the CPG-I film changed noticeably due to the addition of GA, which had a smooth, uniform surface similar to the CP film.[30] Further addition of 3 wt% and 4 wt% GA, *i.e.*, CPG-III and CPG-IV films, resulted in a dense morphology without altering its uniformity, attributed to strong hydrogen bonding interactions between CS, (PVP-*co*-VAc) and GA.[31] However, at higher concentrations of GA, the CPG-IV film showed tiny particles, indicating heterogeneity in the film at higher concentrations, which is attributed to the agglomeration of molecules, leading to stronger intermolecular interactions between GA and the CP polymer matrix.[25]

Bajić M *et al.*[32] and Emma Talón *et al.*[33] obtained similar results, where CS-starch films demonstrated uniform and smooth surfaces because of compatibility in blend solutions. CS/(PVP-*co*-VAc)/GA interactions showed improved tensile strength upon addition of GA in the film in comparison with the CP film. Overall, the addition of GA resulted in changes in the mechanical properties. In the presence of GA, there is a decrease of free volume in the polymer matrix and increased rigidity due to CS/(PVP-*co*-VAc)/GA hydrogen bonding interactions. Ahmed J. *et al.*[34] obtained similar findings: addition of graphene oxide (GO) to the PLA/PEG polymer matrix resulted in increased tensile properties and decreased EB values.

3.3. Atomic force microscopy (AFM)

The surface roughness of GA crosslinked films was analyzed qualitatively with the help of AFM images. As observed from SEM images, all the films possess a dense structure without pores. The AFM images of GA crosslinked CS/(PVP-*co*-VAc) films are shown in Fig. 4. The CP film shows a moderately rough surface without cracks and pores. The addition of 1 wt% GA into the CS/(PVP-*co*-VAc) polymer matrix results in a small change in surface roughness. However, further addition of 2 wt% and 3 wt% GA makes the film homogeneous with some peaks and valleys.

This is due to the intermolecular interactions between GA and the CS/(PVP-*co*-VAc) polymer matrix, which result in reduction of free volume; thus, shortening of the polymer chain takes place, leading to changes in structural arrangements.[35] Similar results were obtained by Jie Liu *et al.*[36] when citric acid was added to soluble soybean polysaccharide films. At a higher GA concentration of 4 wt%, the film shows a heterogeneous and rougher surface morphology. This increased surface roughness upon the addition of GA is mainly attributed to the agglomeration of GA molecules due to the presence of higher concentration of GA.[37] The surface roughness images were also supported by the SEM images.

3.4. X-ray diffraction (XRD) pattern analysis

The crystalline or amorphous nature of the film was investigated using the X-ray diffraction (XRD) technique. The XRD patterns of the CP, CPG-I, CPG-II, CPG-III, and CPG-IV films

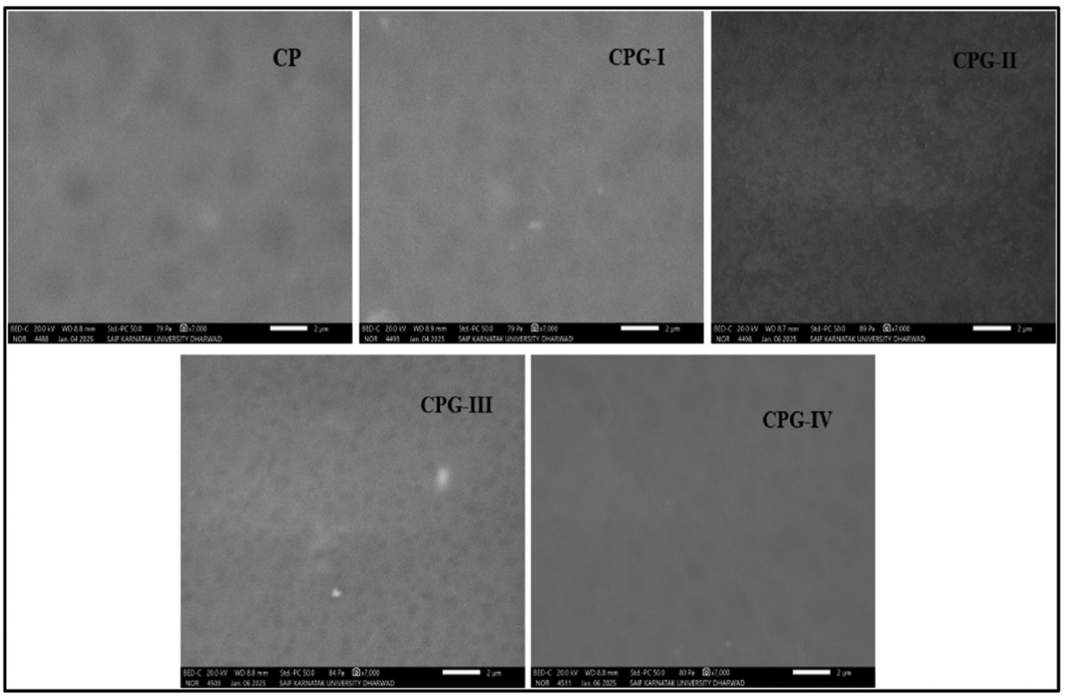

Fig. 3 SEM images of GA crosslinked CS/(PVP-*co*-VAc) films.

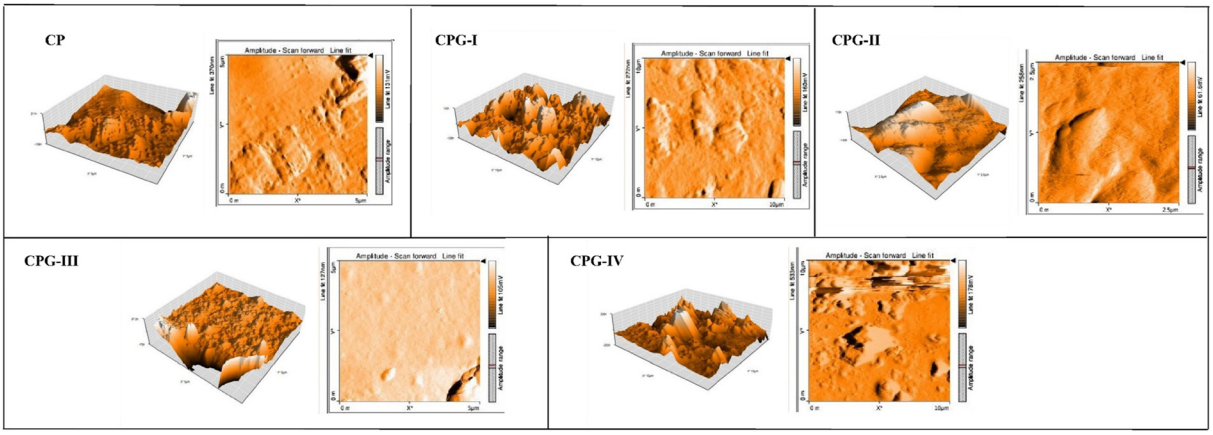

Fig. 4 AFM images of GA crosslinked CS/(PVP-*co*-VAc) films.

are given in Fig. 5(a). In the CP film, the crystalloid and semi-crystalline nature of (PVP-*co*-VAc) and CS was proved by the appearance of distinct peaks at about 22° and 11.45° with a crystallinity of 19.21992% ± 0.5745 respectively.[38] It was found that the peak intensity increased on adding GA, attributed to the homogeneous distribution of GA in the film.[22] The results tabulated in Table 2 show that the CP film without GA has the lowest crystallinity of 19.219% ± 0.5745 compared to the CPG-I, CPG-II, CPG-III, and CPG-IV films. Meanwhile, increasing the GA concentration leads to increased crystallinity.

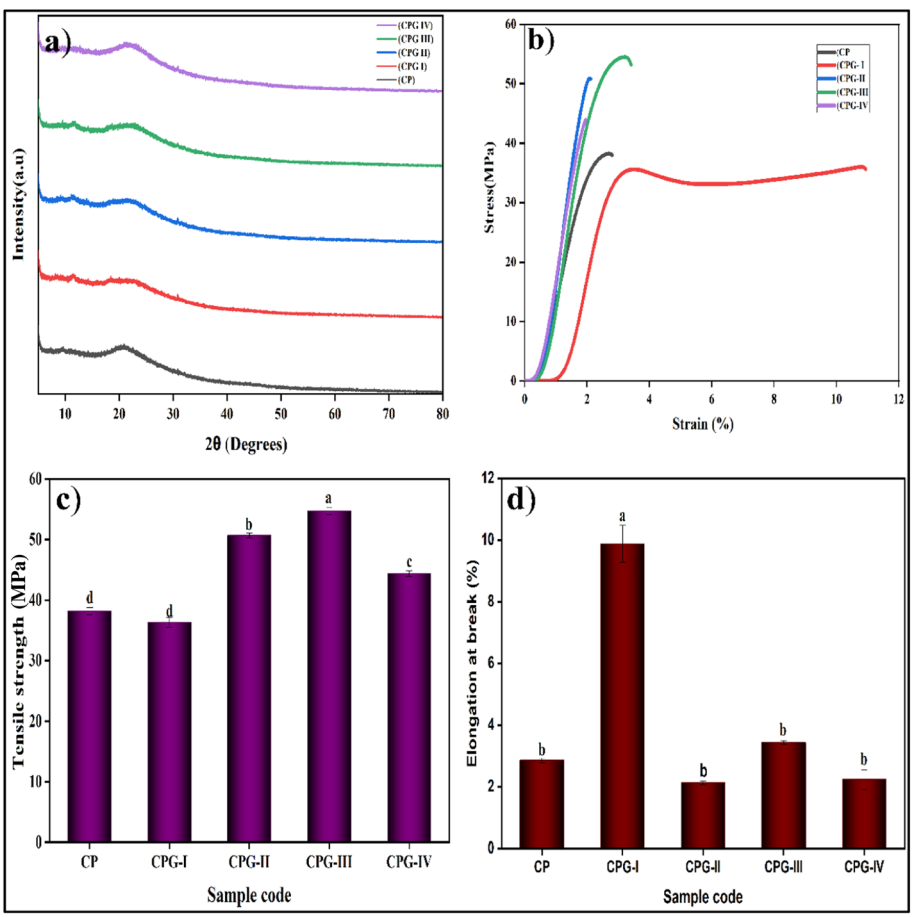

Fig. 5 (a) X-ray diffraction patterns, (b) stress–strain curves, (c) tensile strength values and (d) elongation at break values of GA crosslinked CS/(PVP-*co*-VAc) films.

Table 2 Mechanical properties of gallic acid (GA) crosslinked CS/(PVP-*co*-VAc) films

Sample code	Thickness (mm)	Tensile strength (MPa)	Extensibility (%)	Elastic moduli (MPa)	Crystallinity (%)
CP	0.0506 ± 0.0052[a]	38.172 ± 0.5872[d]	2.861 ± 0.0701[b]	1298.583 ± 0.7084[e]	19.2199 ± 0.5745[e]
CPG-I	0.0403 ± 0.0060[a]	36.334 ± 0.8117[d]	9.879 ± 0.5893[a]	1658.585 ± 0.7362[d]	27.3072 ± 0.5115[d]
CPG-II	0.0521 ± 0.0052[a]	50.657 ± 0.4116[b]	2.127 ± 0.0560[b]	1966.891 ± 0.7592[a]	31.5225 ± 0.4839[c]
CPG-III	0.0523 ± 0.0067[a]	54.713 ± 0.6238[a]	3.438 ± 0.0692[b]	1847.644 ± 0.7136[b]	41.5671 ± 0.5230[b]
CPG-IV	0.0513 ± 0.0052[a]	44.373 ± 0.4388[c]	2.239 ± 0.3208[b]	1749.796 ± 0.4804[c]	48.6523 ± 0.5780[a]

[a–e] Values in the respective columns differ significantly ($p < 0.05$).

This is accounted for by the strong bonding interaction between hydroxyl groups present in the CS/(PVP-*co*-VAc) matrix and GA.[39] The addition of GA led to an increase in peak intensity as depicted in Fig. 5(a). This suggests that GA is responsible for the alterations in the film structure brought about by the interaction with the CS/(PVP-*co*-VAc) matrix. However, GA-related peaks were not clearly seen in XRD, which could be due to the strong interactions, resulting in the overlapping of the GA peaks.[22] The CPG-IV film exhibited an increased crystallinity of 48.65% ± 0.57 in comparison with the CP film. Increased crystallinity also resulted in a more brittle film with less flexibility,[40] which is also supported by the mechanical results, where the CPG-IV film showed a minimum flexibility of 2.23% ± 0.320.

3.5. Thickness and mechanical properties

The tensile strength (TS), elongation at break (EB), and Young's modulus (YM) of films are dependent on the thickness of the film.[41] The GA-incorporated CS/(PVP-*co*-VAc) films showed uniform thickness, indicating homogeneity between CS/(PVP-*co*-VAc) and GA as supported by the FTIR/SEM/XRD results.

Good mechanical properties are necessary for packaging materials to resist stress during transit and storage, lowering damage and scratches.[42] Hence, the mechanical characteristics like TS, EB, and YM were studied, and the results are given in Table 2. These findings demonstrated that the GA-added films showed more tensile strength compared to the CP film. The CP film exhibited a tensile strength of 38.172 ± 0.5872 MPa and a YM of 1298.583 ± 0.7084 MPa. The added GA resulted in increased TS and YM. This increment is attributed to strong bonding interactions between the NH_3^+ of the CS backbone and the OH^- of the GA molecules in the polymer matrix.[43] Similar findings were obtained by Chunnhua Wu *et al.*[44]

The TS and YM values of the films were increased due to the addition of GA; however, at high concentrations, the films showed scattered white patches of GA, leading to a lowering of TS and increased brittleness due to disruption in polymeric chains.[45]

Also, elongation at break is responsible for the nature of a packaging material. The CP film had an EB of 2.861 ± 0.0701%. Initially, the CPG-I film (with a 1 wt% concentration of GA) showed an EB of 10.954%. Additionally, the free voids available in the film reinforce the movement of polymeric chains, consequently increasing the plasticizing and hydrophilic effects (the extensible character) as observed by the decreased WCA in CPG-I. These findings were also similar to observations made by Promsorn J *et al.*[46] The increased EB value upon the addition of 1 wt% GA indicated decreased rigidity of components accountable for the plasticizing nature of GA. However, the crosslinking effect of GA decreases the free volume in the films, giving a more rigid structure by restricting chain mobility; thus the films showed less extensible behavior at high concentrations of GA.[45] The prepared films exhibited enhanced mechanical properties compared with other polymer films, as summarized in Table 7.

3.6. Water contact angle (WCA) measurements

The surface adhesivity could be studied with the help of contact angle measurements. Generally, films show hydrophilic and hydrophobic nature when WCA < 65° and WCA > 65°, respectively.[47] The results are shown in Fig. 6. The CP film revealed surface hydrophilicity with a WCA of 52.6°. This is attributable to the hydrophilic nature of (PVP-*co*-VAc). The lower WCA in the CP film is due to the availability of free –OH groups in the CP film.[48]

Initially, the free –OH groups on the CPG-I film surface lead to increased hydrophilicity.[49] However, it was found that the further addition of 3 wt% of GA to the CP film (CPG-III film) resulted in an enhanced WCA of up to 93.4° and the film became highly hydrophobic in nature. Although GA is hydrophilic, its addition might lead to hydrogen bonding interactions with the matrix. These interactions could result in GA being embedded within the film matrix rather than being exposed at the surface. Consequently, its integration into a crosslinked network might reduce polar functional groups, making them no longer available for water interaction, and the increased crosslinking density also results in reduced free volume and chain mobility, limiting water diffusion.[50]

Thus, a higher WCA of the CPG-III active film makes it a good packaging material. Indeed, the CPG-IV film demonstrated a WCA of 72.7°. This decrease is due to the presence of free –OH groups as a consequence of the higher concentration of GA. These outcomes were supported by the mechanical results.

3.7. Optical parameters

The external appearance of food packaging films is necessary, and it depends on the color of the film. The appearance of the CS/(PVP-*co*-VAc) film was significantly altered by the addition of GA. The CP film appeared in a pale yellow color. When GA was added to the film, its transparency decreased, and the film

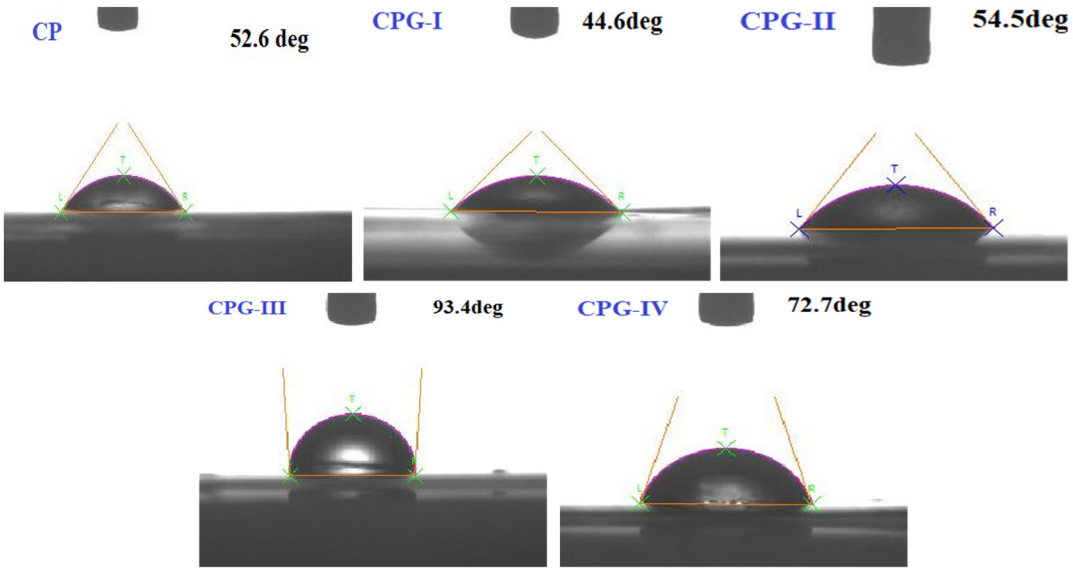

Fig. 6 Water contact angle images of GA crosslinked CS/(PVP-*co*-VAc) films.

became darker. This color change is due to the occurrence of ionic interactions as a result of crosslinking between GA and the NH_2 groups of chitosan.[51]

Food quality and appearance will be affected when UV and visible light interacts with food, causing secondary reactions in vitamins, proteins, *etc*.[52] Thus, it is necessary for packaging materials to possess a property that prevents UV light transmittance. Fig. 7(b) and (c) show that the CP film exhibited percentage transmittance values of 56.77% in the UV region of 380 nm and 37.829% ± 0.04461 at 600 nm. The addition of GA led to a decrease in both transparency and transmittance. The 1 wt%, 2 wt%, 3 wt%, and 4 wt% GA-incorporated films showed decreased percentage transmittance values at 380 nm of 6.63%, 13.32%, 4.47% and 0.9472% respectively. Also, the T_{600} values decreased up to 33.5235% ± 0.06144 in the CPG-IV film. The significant decreases in percentage transmittance and T_{600} were due to the improved interaction between polyphenolic GA chains and chitosan moieties, resulting in a denser network, thus blocking the penetration of UV light.[53] Prodpran T *et al.* obtained similar findings: decreased transmittance and transparency with increased concentrations of polyphenolic compounds like ferulic acid, catechin, caffeic acid, and tannic acid due to the cross-linkage of different compounds with the polymer matrix.[54]

The opacity of the GA-incorporated films was measured at 600 nm wavelength, as shown in Fig. 7(d). The CP film exhibited an opacity of 2.180% ± 0.00997. However, the CPG-IV film showed an increased opacity of 6.4725% ± 0.00642, indicating less UV-light transmittance due to the formation of a dense network.[55]

3.8. Hydration properties

The outcomes of water absorption capacity and water solubility (WS) tests of GA-incorporated films are presented in Fig. 8(a) and (b), respectively, and the findings are summarized in Table 3. The CP film had a water solubility of 29.18% ± 0.605. The addition of 1 wt% GA resulted in a maximum WS of 29.16% ± 0.600 in comparison with the other GA crosslinked films due to the presence of multiple hydroxyl groups in GA. However, on addition of 2 wt% and 3 wt% GA, the film showed improved water solubility values of 20.57% ± 0.564 and 11.43% ± 0.464 respectively. The CPG-III film showed a higher water resistance property, which was also proven by the water contact angle results. The CPG-III film exhibited a hydrophobic nature with WCA = 93.4°. This is attributed to the crosslinking effect of GA, which significantly increases the resistance to water solubility and water absorption capacity, forming a compact crosslinked network, which decreases the availability of free OH groups due to polymer–polymer interactions.[56] Shuwa Bhowmik *et al.* obtained the same findings: the addition of glycerol, chitooligosaccharides, and GA into the chitosan matrix resulted in decreased water solubility.[57] In contrast to this, the CS film showed increased WS values of 32.56% and 34% upon the incorporation of GA and salicylic acid,[58,59] respectively. The CPG-IV film with 4 wt% GA content showed a WS of 14.43% ± 0.578; this is because the added GA leads to a greater number of free hydroxyl groups interacting with water molecules, thus enhancing the WS, owing to the presence of a high concentration of GA; these findings were further supported by the decreased WCA in the CPG-IV film.

Also, the CP film had a water absorption capacity of 95.283% ± 0.535, showing its hydrophilic nature. Addition of 1 wt% and 2 wt% GA resulted in reduced water absorption capacity. This is accountable for the formation of strong bonding interactions between –OH and $–NH_2$ groups on the chitosan surface, reducing the availability of free hydroxyl groups and thereby disturbing the hydrogen bonding in the polymer matrix.[60]

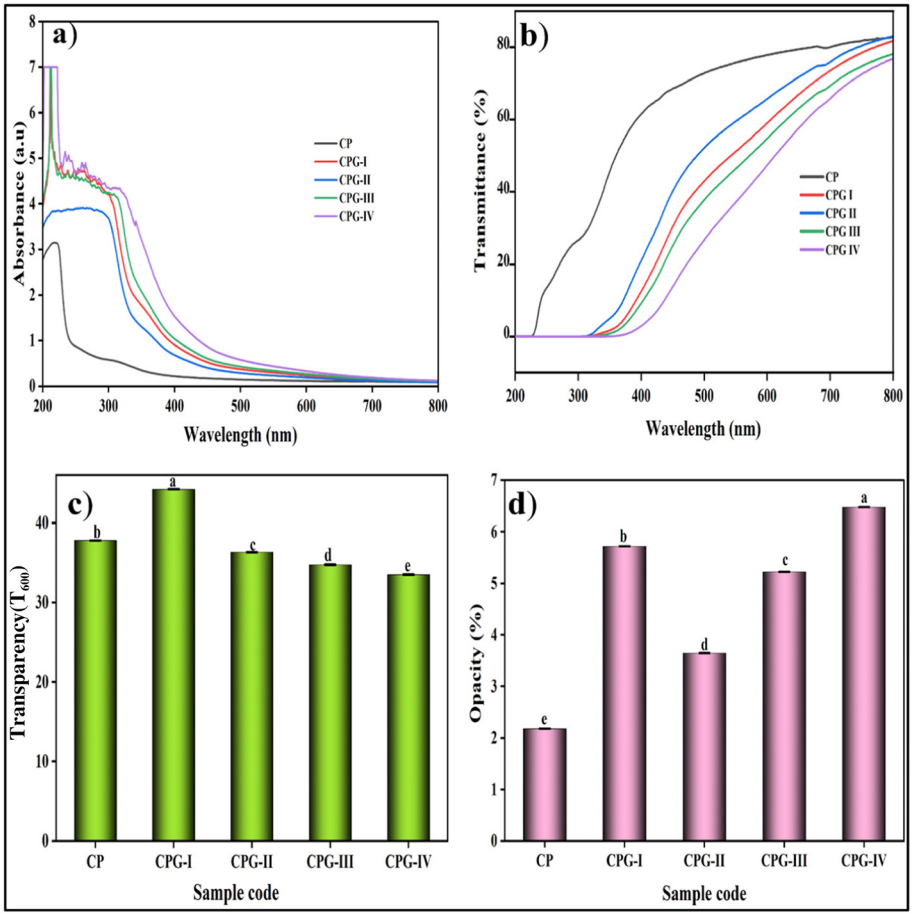

Fig. 7 Optical parameters: (a) absorbance, (b) % transmittance, (c) transparency, and (d) opacity of GA crosslinked CS/(PVP-*co*-VAc) films.

However, the CPG-III film showed the lowest water absorption capacity of 60.356% ± 0.557, and addition of GA at the optimum level led to the formation of a compact crosslinked network, thus reducing water uptake.[60] It was found that the CPG-IV film exhibited a slight increase in water absorption capacity of 64.466% ± 0.733 due to the presence of free –OH groups, owing to an increase in the concentration of GA compared to the optimum level. It was also supported by the water contact angle results.

3.9. Barrier properties

The water vapor transmission rate (WVTR) and oxygen permeability (OP) values of CS/(PVP-*co*-VAc) films are given in Fig. 8(c) and (d) respectively. The CP film has a WVTR of 26.367 ± 0.382 g m^{-2} h. However, addition of GA into the CS/(PVP-*co*-VAc) polymer matrix initially increased the WVTR value in the CPG-I film to 28.295 ± 0.581 g m^{-2} h, which allows penetration of water molecules because of the formation of small pores due to a slight decrease in intermolecular hydrogen bonding interaction between polymeric chains.[61] When the GA concentration was increased, the WVTR values of the CPG-II, CPG-III, and CPG-IV films declined to 25.416 ± 0.425 g m^{-2} h, 25.397 ± 0.835 g m^{-2} h and 24.751 ± 0.307 g m^{-2} h, respectively, compared to that of the CP film. This reduction is accounted for by the restriction of the micro-passages between the CS/(PVP-*co*-VAc) matrix by forming a dense structure due to the crosslinking effect of GA.[62] This formation of dense morphology is supported by SEM images. Bhowmik S *et al.*[57] observed similar findings when GA and chitooligosaccharides were added to the CS polymer matrix.

The disruption in the OP of the film could be due to the changes in the structural arrangement and number of voids present in the polymeric matrix. The OP of the fabricated films indicated that the CP control film showed the highest OP value of 2.574 × 10^{-5} ± 0.067 cc per m per 24 h per atm. However, the addition of GA into the CS/(PVP-*co*-VAc) polymer matrix caused a decrease of the OP value to 1.325 × 10^{-5} ± 0.067 cc per m per 24 h per atm in the CPG-IV film.

The decrease in the diffusive path for oxygen molecules to pass across the CS/(PVP-*co*-VAc) film was the cause of this elevated OP.[63] Also, the addition of GA leads to a more compact structure by accumulating the voids through the cross-linkage between GA and the polymer blend matrix resulting in reduced void volume and OP values through the formation of intermolecular hydrogen bonds.[64] From the literature survey, it is clear that the present WVTR and OP values of the films are in a good range and the films could be effectively used in food packaging applications.[65]

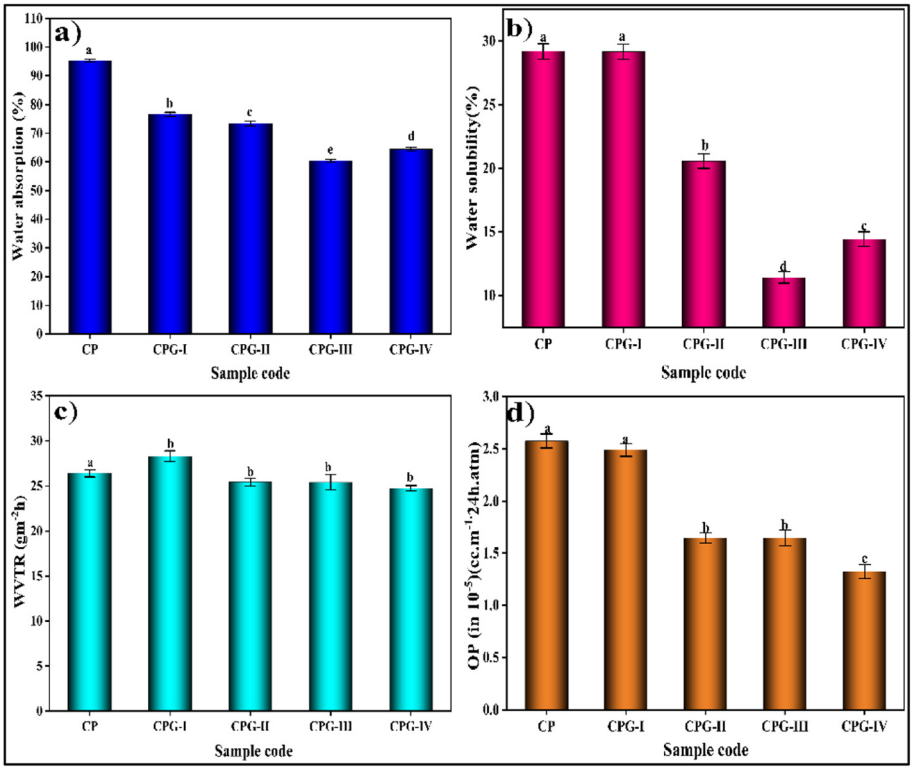

Fig. 8 (a) Water absorption, (b) water solubility, (c) water vapor permeability and (d) oxygen permeability values of GA crosslinked CS/(PVP-*co*-VAc) films.

Table 3 Water solubility, water absorption, water vapor permeability, and oxygen permeability of GA crosslinked CS/(PVP-*co*-VAc) films

Sample code	W_s (%)	W_a (%)	WVTR (g m^{-2} day)	OP (in 10^{-5}) (cc per m per 24 h per atm)
CP	29.18 ± 0.605[a]	95.283 ± 0.535[a]	26.367 ± 0.382[a]	2.574 ± 0.067[a]
CPG-I	29.16 ± 0.600[a]	76.59 ± 0.716[b]	28.295 ± 0.581[b]	2.486 ± 0.060[a]
CPG-II	20.57 ± 0.564[b]	73.37 ± 0.859[c]	25.416 ± 0.425[b]	1.645 ± 0.050[b]
CPG-III	11.43 ± 0.464[d]	60.356 ± 0.557[e]	25.397 ± 0.835[b]	1.645 ± 0.075[b]
CPG-IV	14.43 ± 0.578[c]	64.466 ± 0.733[d]	24.751 ± 0.307[b]	1.325 ± 0.067[c]

[a–e]Values in the respective columns differ significantly ($p < 0.05$).

3.10. Differential scanning calorimetry

Fig. 9 shows the DSC thermograms of GA crosslinked CS/(PVP-*co*-VAc) films. Table 4 presents the glass transition temperature (T_g), melting temperature (T_m) and decomposition temperature (T_d) values of the films. It was observed that all the films showed a single glass transition temperature. The CP film showed a T_g of 88.59 °C. However, in the GA crosslinked films, the glass transition temperature increased to 92.93 °C. This is attributed to the strong interactions of GA with the CS/(PVP-*co*-VAc) polymer matrix, resulting in reduced free volume and chain mobility.[66]

The glass transition temperature values above room temperature indicate that all the films are thermally stable for packaging applications. These higher values are beneficial for increasing the tensile strength of the films, as supported by the mechanical properties. The endothermic peaks around

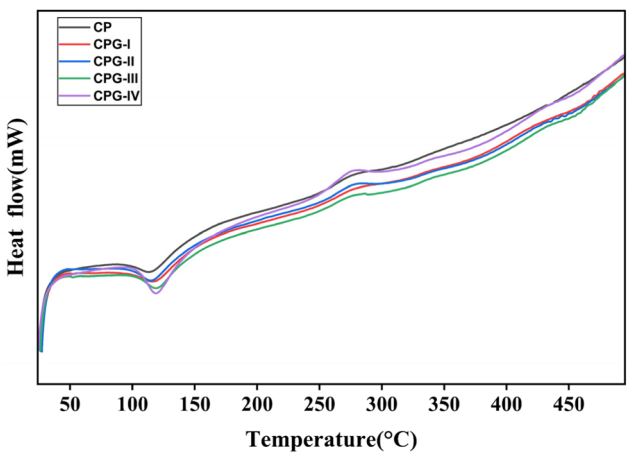

Fig. 9 DSC thermograms of GA crosslinked CS/(PVP-*co*-VAc) films.

Table 4 Glass transition temperature (T_g), melting temperature (T_m) and decomposition temperature (T_d) of GA crosslinked CS/(PVP-*co*-VAc) films

Sample code	Glass transition temperature (T_g) (°C)	Melting temperature (T_m) (°C)	Decomposition temperature (T_d) (°C)
CP	88.59	135.94	308.69 (°C)
CPG-I	88.98	144.71	304.44 (°C)
CPG-II	90.76	140.76	303.95 (°C)
CPG-III	92.93	147.73	309.45 (°C)
CPG-IV	91.65	149.58	302.03 (°C)

135 °C to 149 °C in the DSC thermograms correspond to the melting temperatures of the films due to the loss of moisture content from the films.[67] Increase in the melting temperature on addition of GA suggests that the prepared films were resistant to deformation during high temperature packaging applications.[35] The thermograms of the GA crosslinked films demonstrate that decomposition of the films occurs above T_g and T_m, indicating that the films are stable for food packaging applications. Furthermore, these results indicate that the developed films exhibit sufficient thermal stability requirements for packaging applications in accordance with the FDA guidelines and EU regulation no. 10/2011.

3.11. Titration of free amine groups

The titration of free amine groups using acid–base titration helps to quantify the effect of GA crosslinking in the CS/(PVP-*co*-VAc) blend films (Fig. 10). It was observed that initially the CP film had 0.52 ± 0.008 mmol g^{-1} of free amines. On addition of 1 wt% and 2 wt% GA, free amines underwent crosslinking with –OH groups present in GA, thus showing amine group reduction of 34.61% and 54.61% respectively. Also, the CPG-III film showed the presence of the lowest amount of amino groups (0.09 mmol g^{-1}), due to the loss of titratable amine groups, providing strong evidence for crosslinking. On addition of 4 wt% GA content, the free amine concentration increased to 0.14 mmol g^{-1}. This is attributed to the saturation of free amine groups and altered molecular interactions within the polymer matrix.[68] This slight decrease in crosslinking at higher concentrations of GA was further supported by the tensile strength values and water contact angle findings.

3.12. Overall migration test

The overall migration studies were carried out at 40 °C for 10 days using three stimulants, *viz.* distilled water, alcohol (50%) and acetic acid (3%) representing aqueous media, alcoholic beverages and acidic foods respectively. The test was mainly carried out to assess the extent of sample migration into all three food stimulants. According to the Food Safety and Standards Authority of India 2018 (FSSAI), the permissible migration limit was 10 mg dm^{-2} of food sample. The findings of the present migration studies are given in Table 5. The CP film showed higher migration levels in distilled water and in acetic acid due to the hydrophilic nature and solubility of CS in acetic acid.[69] It was observed that the addition of GA into the film limits the migration of the sample into distilled water, 3% acetic acid and 50% alcohol. This is attributed to the crosslinking of GA molecules between CS and the (PVP-*co*-VAc) polymer matrix; these interactions restrict the chain mobility and diffusion of low molecular fragments into the food stimulants, thus increasing the migration stability.[70]

3.13. Antimicrobial properties

The benefits of the antimicrobial activity of the films are the retardation of population growth of microbes over time and the avoidance of the contamination of microbes entering into

Table 5 Overall migration studies of GA crosslinked CS/(PVP-*co*-VAc) films

	Overall migration as per IS: 9845-1998		
Sample code	Deionised water (mg dm^{-2})	3% acetic acid (mg dm^{-2})	50% alcohol (mg dm^{-2})
CP	4.24 ± 0.01^{a}	2.50 ± 0.05^{a}	2.53 ± 0.12^{a}
CPG-I	1.12 ± 0.03^{bc}	1.21 ± 0.04^{bc}	0.73 ± 0.32^{b}
CPG-II	0.75 ± 0.33^{c}	0.74 ± 0.32^{c}	1.12 ± 0.038^{b}
CPG-III	1.12 ± 0.06^{bc}	1.09 ± 0.05^{bc}	1.38 ± 0.06^{b}
CPG-IV	1.82 ± 0.08^{b}	1.52 ± 0.06^{b}	1.31 ± 0.06^{b}

[a–e]Values in the respective columns differ significantly ($p < 0.05$).

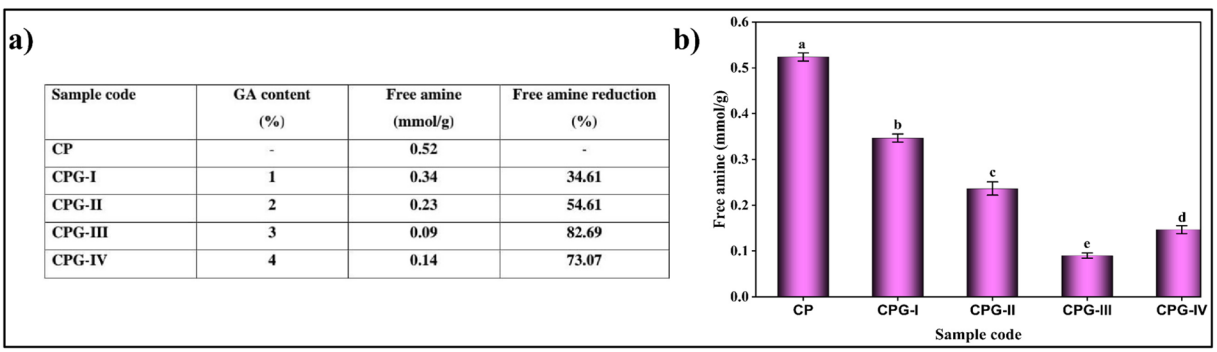

Fig. 10 (a) Table showing free amine content and amine reduction values and (b) graph showing free amine contents in GA crosslinked CS/(PVP-*co*-VAc) films.

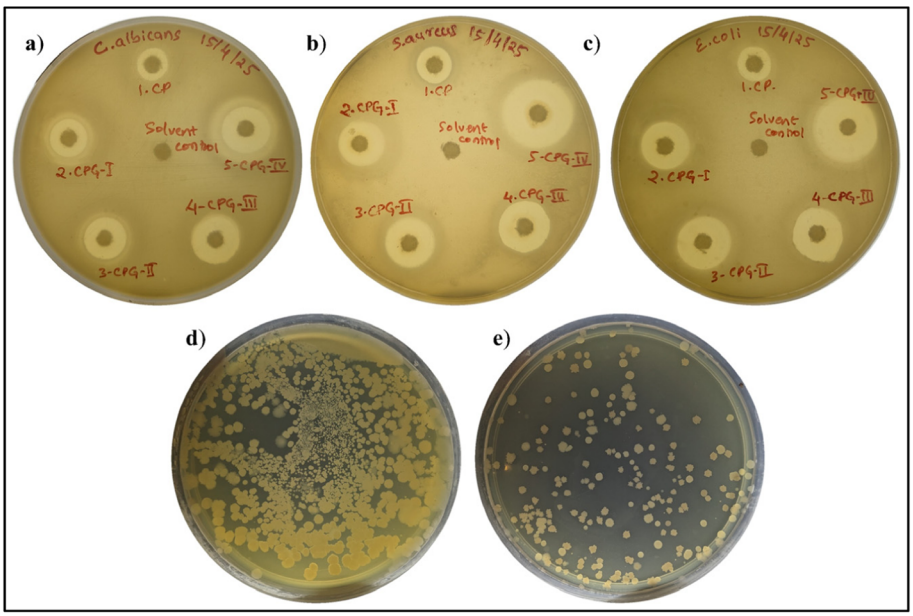

Fig. 11 Microbial growth inhibition profiles of the prepared biofilms against (a) *E. coli*, (b) *S. aureus* and (c) *C. albicans*, and (d) total bacterial count of unpacked chillies and (e) total bacterial count of chillies packed with the CPG-IV film.

food products.[71] The antimicrobial activity of CP films is illustrated in Fig. 11, and the respective zone of inhibition values are tabulated in Table 6. The antimicrobial properties of the prepared films were tested against Gram positive bacteria (*S. aureus*), Gram negative bacteria (*E. coli*) and *C. albicans* fungi.

It was found that all the films exhibited strong antimicrobial properties. This is due to the inherent antimicrobial potential of CS. However, (PVP-*co*-VAc) was not effective against microorganisms. The reason behind the antibacterial activity of CS was the interaction of cationic groups in CS with anionic cell walls in bacteria, resulting in the accumulation of proteinaceous substances inside the cell, which ultimately causes the death of an organism.[72] The presence of a porous permeable peptidoglycan layer in *S. aureus* allows easy entry of antimicrobial agents, leading to a larger zone of inhibition compared to Gram negative bacteria.[73] Additionally, incorporation of GA into the CS/(PVP-*co*-VAc) polymer matrix improved the antimicrobial properties of the fabricated biofilms. This is attributed to the excellent antibacterial properties of GA, where disruption of microbial membranes and denaturation of proteins by GA lead to the leakage of cellular contents, thereby hampering bacterial growth.[74]

Food packaging films also deteriorate due to fungal infestation. The CP film showed good antifungal activity. In addition to this, the increase in the weight percentage of GA also results in enhanced inhibition zones against *C. albicans*. It was found that CPG exhibited an increased zone of inhibition value of 17.66 ± 0.635 mm from 9.36 ± 0.806 mm. It is higher than those of chitosan–HPMC films reported by Gunaki *et al.*[75] and Ch–CMC blend films (19.31 mm) reported by Noshirvani N *et al.*[76] In both antibacterial and antifungal studies, the films act as effective barriers for microbes by preventing growth and damage to the DNA through rupture of the membrane, ultimately resulting in the death of the pathogen. The incorporation of GA into the CS/(PVP-*co*-VAc) polymer matrix endowed it with good antimicrobial activity in comparison with the CP film, making it appropriate for packaging applications.

Table 6 Antimicrobial inhibition zones (in mm) of the CP (control) and CPG-I, CPG-II, CPG-III, and CPG-IV films

Sample name	Zone of inhibition (mm)		
	E. coli	*S. aureus*	*C. albicans*
CP	10.62 ± 0.398^{e}	10.58 ± 0.584^{d}	9.36 ± 0.806^{d}
CPG-I	15.68 ± 0.624^{d}	15.23 ± 0.646^{c}	12.32 ± 0.836^{cd}
CPG-II	17.63 ± 0.603^{c}	17.55 ± 0.522^{bc}	14.16 ± 0.545^{bc}
CPG-III	18.08 ± 0.557^{b}	19.22 ± 0.516^{b}	16.53 ± 0.513^{ab}
CPG-IV	22.23 ± 0.506^{a}	22.12 ± 0.620^{a}	17.66 ± 0.635^{a}

[a–e]Values in the respective columns differ significantly ($p < 0.05$).

3.14. Antioxidant properties

It is of immense importance to prevent food components such as protein and lipid molecules from oxidation by using packaging materials. Lipid molecules, on interaction with oxygen, result in the generation of free radicals, which cause loss of quality and appearance of food.[77] Antioxidant packaging materials help in extending the quality of food. This antioxidant capacity is determined using the DPPH assay. Fig. 12(b) shows less antioxidant activity of the CP film. Addition of GA into the polymer matrix led to increased antioxidant activity, which is accounted for by the free radical interaction with GA through the radical polymerization process by an electron transfer mechanism.[78]

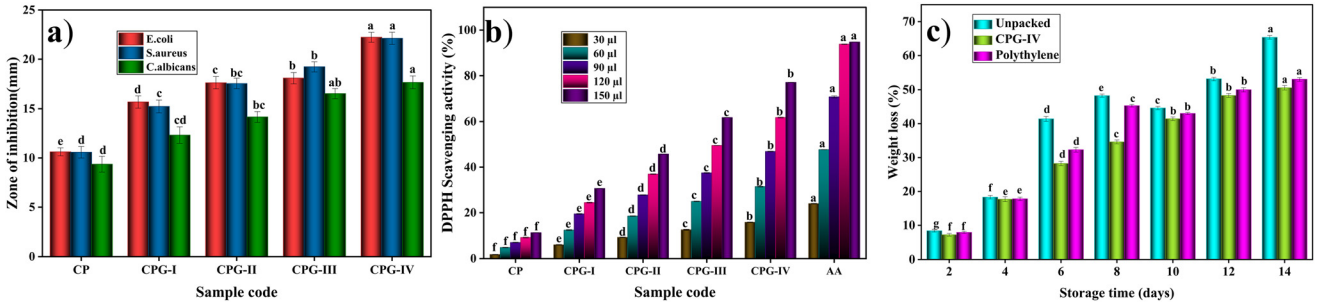

Fig. 12 (a) Antimicrobial activity profiles of the films, (b) antioxidant activity profiles of the films and (c) physiological weight loss (%) values of GA crosslinked CS/(PVP-*co*-VAc) films.

The CPG-IV film demonstrated a higher antioxidant potential compared to the other films, owing to the presence of a high concentration of –OH functional groups on the surface of the film due to the addition of 4 wt% GA. The enhanced concentration of hydroxyl groups increases the shift of electrons, thus promoting the free radical scavenging phenomenon.[79] Thus, it is evident that GA-incorporated films showed antioxidant activity in comparison with the CP film, making them better materials in antioxidant packaging applications.

3.15. Packaging efficiency

Chillies are generally considered to be one of the widely used vegetables in day-to-day life. Fresh chillies are highly prone to physical damage, moisture loss, and microbial attack. Thus, the packaging study involves the extension of shelf life by the incorporation of strong antimicrobial agents. Chillies are widely available throughout the year, which makes them convenient for study as a packaged material. The CPG-IV film was chosen for the packaging study among all other films, because, in contrast to the other films, it has good antimicrobial and antioxidant properties. The packaging efficiency of the CPG-IV film was studied in comparison with the unpacked chillies and chillies packed with a polyethylene film. The physical texture of the green chillies for up to 14 days is shown in Fig. 13. Initially, every packed and unpacked chilli was green in appearance; then, the unpacked chilli started to lose its green color and became deteriorated during the time period of 14 days. Also, the unpacked chilli shrank and underwent a dehydration process due to water loss.[80] The chilli packed with polyethylene shrank on the 14th day of storage. In contrast, the CPG-IV film retained the chilli's physical appearance after 14 days of storage. This is due to the high antioxidant activity of the CPG-IV film, which hampers the generation of free radicals, thus stopping the oxidation of components in the chilli.

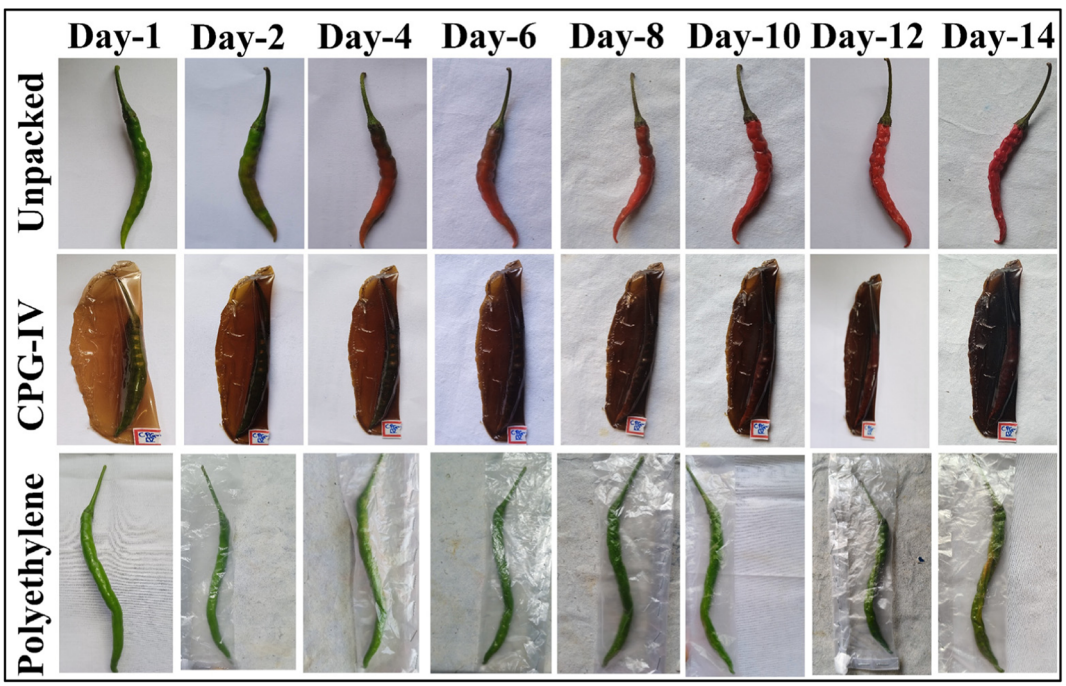

Fig. 13 Visual appearance of unpacked and packed chillies.

Table 7 Comparison of the mechanical, biodegradability and cost effective properties of various crosslinking agents incorporated into the different polymer matrices

Sl. no.	Crosslinking agent used	TS (MPa)	EB (%)	Biodegradability	Cost effective	Ref.
1	Tannic acid	4.10 ± 0.26	42.71 ± 8.20	Biodegradable	More expensive	83
2	Citric acid	6.5 ± 0.5	33.9 ± 2.2	Biodegradable	Less expensive	84
3	Citric acid	6.93 ± 0.16	77.76 ± 0.2	Biodegradable	Less expensive	85
4	Vanillin	10.18 ± 0.41	43.73 ± 2.03	Biodegradable	Less expensive	86
5	Tannic acid	11.29 ± 0.22	42.02 ± 4.14	Biodegradable	More expensive	87
6	Caffeic acid	13.97 ± 0.69	34.53 ± 2.80	Biodegradable	More expensive	88
7	Caffeic acid	17.7	219.3	Biodegradable	More expensive	89
8	Citric acid	20.4	677	Biodegradable	Less expensive	90
9	Tannic acid	26.99 ± 1.91	3.65 ± 0.02	Biodegradable	More expensive	91
10	Vanillin	40.1 ± 1.2	30.1	Biodegradable	Less expensive	92
11	Vanillin	43.04 ± 4.8	40.49 ± 4.82	Biodegradable	Less expensive	93
12	Gallic acid	54.71 ± 0.62	3.43 ± 0.06	Biodegradable	Cost effective	Present work

Also, the weight loss values of the unpacked chillies, chillies packed with polyethylene and those packed with the CPG-IV film are shown in Fig. 12(c). It was found that the main reason for weight loss is dehydration through evaporation and cellular respiration. Unpacked chillies showed more weight loss on the 14th day of storage in comparison with those with the CPG-IV film and polyethylene. The chillies packed with the CPG-IV film showed decreased weight loss in comparison with the unpacked chillies on the 14th day of storage. This is attributed to the improved WVTR, OP, and antioxidant properties of the CPG-IV film, which altered the internal atmosphere, thereby avoiding dehydration.[81] Also, the chillies packed with polyethylene showed less weight loss in comparison with the chillies exposed to the environment; this is due to the hydrophobic behavior of the polyethylene bag.[82] Furthermore, the total bacterial count test was determined with the help of Fig. 11(d) and (e). The total bacterial study revealed that the unpacked chillies showed less resistance to bacterial attack in comparison with the chillies packed with the CPG-IV film. This is accountable for the good antibacterial properties of the CPG-IV film, which was also supported by the antibacterial results.

4. Conclusions

The present work mainly focused on using an ecofriendly solvent casting method for the fabrication of polymeric films. FTIR findings clearly explained the formation of hydrogen bonding between GA and the CS/(PVP-*co*-VAc) polymer matrix. Also, SEM studies revealed the formation of dense morphology upon the addition of GA. This addition of GA brought changes in the WS and WCA characteristics and also showed good mechanical and barrier properties. The fabricated films showed potential antibacterial and antioxidant nature upon incorporation of GA into the CS/(PVP-*co*-VAc) polymer matrix. The CPG-IV film exhibited higher antioxidant activity (77.18% ± 0.020) and antimicrobial property than the CP film. In addition to this, the packaging study results showed that the CPG-IV film with 4 wt% of GA maintained the quality of chillies by regulating the weight loss and extending the shelf life of chillies for a period of 14 days. Thus, these findings suggested that GA-incorporated CS/(PVP-*co*-VAc) films could be used in food packaging applications.

Author contributions

Bhagyalakshmi A. Sheeparamatti: conceptualization, data interpretation, formal analysis, writing – original manuscript; Priyanka Baburao: formal analysis, design of the study, data curation; Priyadarshini: formal analysis, data curation; Shiddalingesh G. Havanur: formal analysis, design of the study, data curation; Ravindra B. Chougale: supervision, correspondence, review, formal correction; Manjushree Nagaraj Gunaki: formal analysis, data curation; Ajitkumar Appayya Hunashyal: formal analysis, data curation, investigation; Saraswati P. Masti: revising manuscript; Nagarjuna Prakash Dalbanjan: analysis of data (microbiology part); Praveen Kumar S. K.: review and editing (microbiology part). All authors have read and approved the final manuscript.

Conflicts of interest

The authors declare that they have no known competing financial interests or personal relationships that could have appeared to influence the work reported in this paper.

Data availability

The data will be made available on request.

Acknowledgements

The authors also express their gratitude to the Head of the Department of Chemistry, Karnatak University, Dharwad-580003, for providing infrastructure facilities. All authors are grateful to DST SERB for aid provided for purchase of the UTM (Dr Saraswati P. Masti, principal investigator, under project sanction letter no. SB/EMEQ-213/2014, dated: 29-1-2016) for

measurements of mechanical characteristics. The authors sincerely acknowledge the University Scientific Instrumentation Centre (USIC) and SAIF, Karnatak University, Dharwad, for providing the instrumental facilities.

References

1 E. Akanele, S. M. O. Chukwu and C. M. Ahudie, *Int. J. Sci. Technol. Res.*, 2016, **5**(3), 65–78.
2 S. Khandeparkar, R. Paul, A. Sridhar, V. V. Lakshmaiah and P. Nagella, *Sustainable Chem. Pharm.*, 2024, **39**, 101579, DOI: 10.1016/j.scp.2024.101579.
3 P. Lata Meena, A. Goel, V. Rai, E. S. Rao, M. Singh Barwa and C. Manjeet Singh Barwa, *Int. J. Appl. Res.*, 2017, **3**, 886–896.
4 S. Sid, R. S. Mor, A. Kishore and V. S. Sharanagat, *Trends Food Sci. Technol.*, 2021, **115**, 87–104, DOI: 10.1016/j.tifs.2021.06.026.
5 A. Lestido-Cardama, L. Barbosa-Pereira, R. Sendón, J. Bustos, P. Paseiro Losada and A. Rodríguez Bernaldo de Quirós, *Food Res. Int.*, 2025, **202**, 115737, DOI: 10.1016/j.foodres.2025.115737.
6 M. Ferri, K. Papchenko, M. Degli Esposti, G. Tondi, M. G. De Angelis, D. Morselli and P. Fabbri, *ACS Appl. Mater. Interfaces*, 2023, **15**, 28594–28605, DOI: 10.1021/acsami.3c04611.
7 S. R. Kanatt, M. S. Rao, S. P. Chawla and A. Sharma, *Food Hydrocolloids*, 2012, **29**, 290–297, DOI: 10.1016/j.foodhyd.2012.03.005.
8 P. Singh, V. K. Pandey, R. Singh, K. Singh, K. K. Dash and S. Malik, *J. Agric. Food Res.*, 2024, **15**, 101065, DOI: 10.1016/j.jafr.2024.101065.
9 A. A. Hunashyal, S. P. Masti, L. K. Kurabetta, M. N. Gunaki, S. Madihalli, J. P. Pinto, M. B. Megalamani, B. Thokchom, R. B. Yarajarla and R. B. Chougale, *Sustainable Food Technol.*, 2025, **3**, 2088–2107, DOI: 10.1039/D5FB00358J.
10 M. N. Gunaki, S. P. Masti, L. K. Kurabetta, S. Madihalli, A. A. Hunashyal, R. B. Chougale, V. Holeyannavar and S. Kumar Vootla, *J. Environ. Chem. Eng.*, 2025, **13**, 118397, DOI: 10.1016/j.jece.2025.118397.
11 S. (Gabriel) Kou, L. M. Peters and M. R. Mucalo, *Int. J. Biol. Macromol.*, 2021, **169**, 85–94, DOI: 10.1016/j.ijbiomac.2020.12.005.
12 P. Kong, S. M. Rosnan and T. Enomae, *Carbohydr. Polym.*, 2024, **346**, 122612, DOI: 10.1016/j.carbpol.2024.122612.
13 F. Bigi, H. Haghighi, H. W. Siesler, F. Licciardello and A. Pulvirenti, *Food Hydrocolloids*, 2021, **120**, 106979, DOI: 10.1016/j.foodhyd.2021.106979.
14 X. Sun, H. Wang, H. Liang, N. Meng and N. Zhou, *Food Hydrocolloids*, 2025, **159**, 110686, DOI: 10.1016/j.foodhyd.2024.110686.
15 W. Yang, J. S. Owczarek, E. Fortunati, M. Kozanecki, A. Mazzaglia, G. M. Balestra, J. M. Kenny, L. Torre and D. Puglia, *Ind. Crops Prod.*, 2016, **94**, 800–811, DOI: 10.1016/j.indcrop.2016.09.061.
16 A. M. Hussein, M. A. Rusho, M. Elangovan, M. A. Diab, A. Abilkasimov, B. Madaminov, Z. Atamuratova, A. Smerat, S. K. Issa, A. I. A. Arabi and S. Islam, *J. Organomet. Chem.*, 2025, **1039**, 123765, DOI: 10.1016/j.jorganchem.2025.123765.
17 S. Ilić-Stojanović, S. Cakić, I. Ristić, M. Kostić, Đ. Petrović, N. Nikolić and S. Petrović, *Adv. Technol.*, 2024, **13**, 35–44, DOI: 10.5937/savteh2402035I.
18 L. M. Martins, G. N. Fraga, M. C. G. Pellá, F. A. C. Pinto, F. de Souza, J. C. Neto, A. R. S. Rossin, J. Caetano and D. C. Dragunski, *Process Biochem.*, 2022, **122**, 8–15, DOI: 10.1016/j.procbio.2022.09.019.
19 Y. Liu, L. Chen, H. Xu, Y. Liang and B. Zheng, *Int. J. Biol. Macromol.*, 2019, **134**, 856–863, DOI: 10.1016/j.ijbiomac.2019.05.083.
20 C. R. Lee, S. J. Lee, T. I. Kim, K. Chathuranga, J. S. Lee, S. Kim, M. H. Kim and W. H. Park, *Food Chem.*, 2025, **463**, 141322, DOI: 10.1016/j.foodchem.2024.141322.
21 S. Bhatia, A. Al-Harrasi, M. S. Al-Azri, S. Ullah, H. A. Makeen, A. M. Meraya, M. Albratty, A. Najmi and M. K. Anwer, *Polymers*, 2022, **14**(19), 4065, DOI: 10.3390/polym14194065.
22 N. Goudar, V. N. Vanjeri, S. Dixit, V. Hiremani, S. Sataraddi, T. Gasti, S. K. Vootla, S. P. Masti and R. B. Chougale, *Int. J. Biol. Macromol.*, 2020, **158**, 139–149, DOI: 10.1016/j.ijbiomac.2020.04.223.
23 W. Gong, T. Q. Yang, W. Y. He, Y. X. Li and J. N. Hu, *Food Chem.*, 2025, **463**, 141404, DOI: 10.1016/j.foodchem.2024.141404.
24 K. Lin, Y. Z. Zhu, H. W. Ma, J. C. Wu, C. N. Kong, Y. Xiao, H. C. Liu, L. L. Zhao, X. L. Qin and L. F. Yang, *Int. J. Biol. Macromol.*, 2024, **277**, 134008, DOI: 10.1016/j.ijbiomac.2024.134008.
25 R. Venkatesan, T. Dhilipkumar, K. V. Shankar, T. M. Almutairi and S. C. Kim, *Cellulose*, 2024, **31**, 8105–8125, DOI: 10.1007/s10570-024-06046-w.
26 M. Zhang, B. Yang, Z. Yuan, Q. Sheng, C. Jin, J. Qi, M. Yu, Y. Liu and G. Xiong, *Food Chem.:X*, 2023, **19**, 100782, DOI: 10.1016/j.fochx.2023.100782.
27 L. K. Kurabetta, S. P. Masti, M. P. Eelager, M. N. Gunaki, S. Madihalli, A. A. Hunashyal, R. B. Chougale, P. S. K. Kumar and A. J. Kadapure, *Int. J. Biol. Macromol.*, 2023, **253**, 127552, DOI: 10.1016/j.ijbiomac.2023.127552.
28 T. Gasti, S. Dixit, V. D. Hiremani, R. B. Chougale, S. P. Masti, S. K. Vootla and B. S. Mudigoudra, *Carbohydr. Polym.*, 2022, **277**, 118866, DOI: 10.1016/j.carbpol.2021.118866.
29 Y. Wu, Y. Ying, Y. Liu, H. Zhang and J. Huang, *Int. J. Biol. Macromol.*, 2018, **118**, 2131–2137, DOI: 10.1016/j.ijbiomac.2018.07.061.
30 L. K. Kurabetta, S. P. Masti, M. N. Gunaki, A. A. Hunashyal, R. B. Chougale, N. P. Dalbanjan and S. K. Praveen Kumar, *Food Biosci.*, 2024, **61**, 104869, DOI: 10.1016/j.fbio.2024.104869.
31 X. Sun, M. Dong, Z. Guo, H. Zhang, J. Wang, P. Jia, T. Bu, Y. Liu, L. Li and L. Wang, *Int. J. Biol. Macromol.*, 2021, **167**, 10–22, DOI: 10.1016/j.ijbiomac.2020.11.153.

32 M. Bajić, T. Ročnik, A. Oberlintner, F. Scognamiglio, U. Novak and B. Likozar, *Food Packag. Shelf Life*, 2019, **21**, 100365, DOI: 10.1016/j.fpsl.2019.100365.
33 E. Talón, K. T. Trifkovic, V. A. Nedovic, B. M. Bugarski, M. Vargas, A. Chiralt and C. González-Martínez, *Carbohydr. Polym.*, 2017, **157**, 1153–1161, DOI: 10.1016/j.carbpol.2016.10.080.
34 J. Ahmed, M. Z. Mulla, A. Vahora, A. Bher and R. Auras, *Food Packag. Shelf Life*, 2021, **29**, 100702, DOI: 10.1016/j.fpsl.2021.100702.
35 D. Kasai, R. Chougale, S. Masti, G. Gouripur, R. Malabadi, R. Chalannavar, A. V. Raghu, D. Radhika, H. Shanavaz and S. Dhanavant, *Green Mater.*, 2020, **9**, 49–68, DOI: 10.1680/jgrma.20.00014.
36 J. Liu, Y. Dong, X. Zheng, Y. Pei and K. Tang, *Food Chem.*, 2024, **438**, 138009, DOI: 10.1016/j.foodchem.2023.138009.
37 I. Karakurt, K. Ozaltin, E. Vargun, L. Kucerova, P. Suly, E. Harea, A. Minařík, K. Štěpánková, M. Lehocky, P. Humpolícek, A. Vesel and M. Mozetic, *Mater. Sci. Eng., C*, 2021, **123**, 112125, DOI: 10.1016/j.msec.2021.112125.
38 J. P. Pinto, V. D. Hiremani, O. J. D'Souza, S. Khanapure, S. S. Narasagoudr, N. Goudar, S. K. Vootla, S. P. Masti and R. B. Chougale, *Food Humit.*, 2023, **1**, 378–390, DOI: 10.1016/j.foohum.2023.06.003.
39 C. M. Zaccaron, R. V. B. Oliveira, M. Guiotoku, A. T. N. Pires and V. Soldi, *Polym. Degrad. Stab.*, 2005, **90**, 21–27, DOI: 10.1016/j.polymdegradstab.2005.02.010.
40 N. Goudar, V. N. Vanjeri, V. D. Hiremani, T. Gasti, S. Khanapure, S. P. Masti and R. B. Chougale, *J. Polym. Environ.*, 2022, **30**, 2419–2434, DOI: 10.1007/s10924-021-02354-5.
41 K. S. Venkataprasanna, J. Prakash, S. Vignesh, G. Bharath, M. Venkatesan, F. Banat, S. Sahabudeen, S. Ramachandran and G. Devanand Venkatasubbu, *Int. J. Biol. Macromol.*, 2020, **143**, 744–762, DOI: 10.1016/j.ijbiomac.2019.10.029.
42 V. D. Hiremani, S. Khanapure, T. Gasti, N. Goudar, S. K. Vootla, S. P. Masti, R. B. Malabadi, B. S. Mudigoudra and R. B. Chougale, *Int. J. Biol. Macromol.*, 2021, **193**, 2192–2201, DOI: 10.1016/j.ijbiomac.2021.11.050.
43 W. Pasanphan and S. Chirachanchai, *Carbohydr. Polym.*, 2008, **72**, 169–177, DOI: 10.1016/j.carbpol.2007.08.002.
44 C. Wu, J. Tian, S. Li, T. Wu, Y. Hu, S. Chen, T. Sugawara and X. Ye, *Carbohydr. Polym.*, 2016, **146**, 10–19, DOI: 10.1016/j.carbpol.2016.03.027.
45 X. Sun, Z. Wang, H. Kadouh and K. Zhou, *LWT – Food Sci. Technol.*, 2014, **57**, 83–89, DOI: 10.1016/j.lwt.2013.11.037.
46 J. Promsorn and N. Harnkarnsujarit, *Food Control*, 2022, **142**, 109273, DOI: 10.1016/j.foodcont.2022.109273.
47 T. Gasti, S. Dixit, O. J. D'Souza, V. D. Hiremani, S. K. Vootla, S. P. Masti, R. B. Chougale and R. B. Malabadi, *Int. J. Biol. Macromol.*, 2021, **187**, 451–461, DOI: 10.1016/j.ijbiomac.2021.07.128.
48 J. E. Patterson, M. B. James, A. H. Forster and T. Rades, *Drug Dev. Ind. Pharm.*, 2008, **34**, 95–106, DOI: 10.1080/03639040701484627.
49 X. Yang, B. Wang, D. Sha, Y. Liu, Z. Liu, K. Shi, W. Liu, C. Yu and X. Ji, *ACS Appl. Polym. Mater.*, 2021, **3**, 3867–3877, DOI: 10.1021/acsapm.1c00447.
50 L. K. Kurabetta, S. P. Masti, M. N. Gunaki, A. A. Hunashyal, M. P. Eelager, R. B. Chougale, N. P. Dalbanjan and S. K. Praveen Kumar, *Int. J. Biol. Macromol.*, 2024, **277**, 134191, DOI: 10.1016/j.ijbiomac.2024.134191.
51 M. Kurek, M. Ščetar, M. Nuskol, T. Janči, M. Tanksoić, D. Klepac, M. Čakić Semenčić and K. Galić, *Antioxidants*, 2024, **13**, 707, DOI: 10.3390/antiox13060707.
52 S. E. Duncan and S. Hannah, in *Emerging Food Packaging Technologies: Principles and Practice*, ed. K. L. Yam and D. S. Lee, Elsevier Ltd, 2012, pp. 303–322, DOI: 10.1533/9780857095664.
53 S. Parveen, P. Chaudhury, U. Dasmahapatra and S. Dasgupta, *Int. J. Biol. Macromol.*, 2019, **139**, 12–20, DOI: 10.1016/j.ijbiomac.2019.07.143.
54 T. Prodpran, S. Benjakul and S. Phatcharat, *Int. J. Biol. Macromol.*, 2012, **51**, 774–782, DOI: 10.1016/j.ijbiomac.2012.07.010.
55 F. J. Leyva-Jiménez, C. Abellán-Dieguez, R. Oliver-Simancas, A. M. Rodríguez-García and M. E. Alañón, *Future Foods*, 2024, **10**, 100464, DOI: 10.1016/j.fufo.2024.100464.
56 A. P. Subramanian, A. A. John, M. V. Vellayappan, A. Balaji, S. K. Jaganathan, E. Supriyanto and M. Yusof, *RSC Adv.*, 2015, **5**, 22727–22734, DOI: 10.1039/c5ra02727f.
57 S. Bhowmik, D. Agyei and A. Ali, *Sustainable Mater. Technol.*, 2024, **41**, e01092, DOI: 10.1016/j.susmat.2024.e01092.
58 G. Singh, S. Singh, B. Kumar and K. K. Gaikwad, *J. Food Meas. Charact.*, 2021, **15**, 585–593, DOI: 10.1007/s11694-020-00669-W.
59 F. Hu, T. Sun, J. Xie, B. Xue, X. Li, J. Gan, L. Li, X. Bian and Z. Shao, *J. Mol. Struct.*, 2020, **1227**, 129237, DOI: 10.1016/j.molstruc.2020.129237.
60 L. Rui, M. Xie, B. Hu, L. Zhou, D. Yin and X. Zeng, *Carbohydr. Polym.*, 2017, **173**, 473–481, DOI: 10.1016/j.carbpol.2017.05.072.
61 L. Nouri and A. Mohammadi Nafchi, *Int. J. Biol. Macromol.*, 2014, **66**, 254–259, DOI: 10.1016/j.ijbiomac.2014.02.044.
62 M. Zhang, B. Yang, Z. Yuan, Q. Sheng, C. Jin, J. Qi, M. Yu, Y. Liu and G. Xiong, *Food Chem.:X*, 2023, **19**, 100782, DOI: 10.1016/j.fochx.2023.100782.
63 G. Singh, S. Singh, B. Kumar and K. K. Gaikwad, *J. Food Meas. Charact.*, 2021, **15**, 585–593, DOI: 10.1007/s11694-020-00669-W.
64 J. P. Pinto, M. H. Anandalli, A. A. Hunashyal, Priyadarshini, S. P. Masti, R. B. Chougale, V. Gudihal and R. F. Bhajantri, *J. Mater. Sci.: Mater. Electron.*, 2025, **36**, 1035, DOI: 10.1007/s10854-025-15058-6.
65 J. Lamarra, S. Rivero and A. Pinotti, *Int. J. Biol. Macromol.*, 2020, **146**, 811–820, DOI: 10.1016/j.ijbiomac.2019.10.049.
66 S. Jiang, C. Qiao, R. Liu, Q. Liu, J. Xu and J. Yao, *Carbohydr. Polym.*, 2024, **311**, 120842, DOI: 10.1016/j.carbpol.2023.120842.

67 N. Goudar, V. N. Vanjeri, S. Dixit, V. Hiremani, S. Sataraddi, T. Gasti, S. K. Vootla, S. P. Masti and R. B. Chougale, *Int. J. Biol. Macromol.*, 2020, **158**, 139–149, DOI: 10.1016/j.ijbiomac.2020.04.223.
68 S. Tanpichai, K. Yuwawech, E. Wimolmala, Y. Srimarut, W. Woraprayote and Y. Malila, *RSC Adv.*, 2025, **15**, 30742–30757, DOI: 10.1039/D5RA04227E.
69 N. Goudar, V. N. Vanjeri, S. Dixit, V. Hiremani, S. Sataraddi, T. Gasti, S. K. Vootla, S. P. Masti and R. B. Chougale, *Int. J. Biol. Macromol.*, 2020, **158**, 139–149, DOI: 10.1016/j.ijbiomac.2020.04.223.
70 T. Gasti, S. Dixit, R. B. Chougale and S. P. Masti, *Sustainable Food Technol.*, 2023, **1**, 390–403, DOI: 10.1039/D3FB00007A.
71 T. Gasti, S. Dixit, L. A. Shastri, B. S. Mudigoudra, R. B. Chougale and S. P. Masti, *ACS Food Sci. Technol.*, 2025, **5**, 2430–2443, DOI: 10.1021/acsfoodscitech.5c00238.
72 R. Priyadarshi and J. W. Rhim, *Innovative Food Sci. Emerging Technol.*, 2020, **62**, 102346, DOI: 10.1016/j.ifset.2020.102346.
73 T. J. Silhavy, D. Kahne and S. Walker, *Cold Spring Harbor Perspect. Biol.*, 2010, **2**(5), a000414, DOI: 10.1101/cshperspect.a000414.
74 Priyadarshini, O. J. D'Souza, J. P. Pinto, V. D. Hiremani, S. P. Masti, N. P. Dalbanjan, S. K. Praveen Kumar and R. B. Chougale, *Food Humit.*, 2025, **5**, 100840, DOI: 10.1016/j.foohum.2025.100840.
75 M. N. Gunaki, S. P. Masti, O. J. D'Souza, M. P. Eelager, L. K. Kurabetta, R. B. Chougale, A. J. Kadapure and S. K. Praveen Kumar, *Food Hydrocolloids*, 2024, **152**, 109937, DOI: 10.1016/j.foodhyd.2024.109937.
76 N. Noshirvani, B. Ghanbarzadeh, C. Gardrat, M. R. Rezaei, M. Hashemi, C. Le Coz and V. Coma, *Food Hydrocolloids*, 2017, **70**, 36–45, DOI: 10.1016/j.foodhyd.2017.03.015.
77 M. Muthu, J. Gopal, S. Chun, A. J. P. Devadoss, N. Hasan and I. Sivanesan, *Antioxidants*, 2021, **10**(2), 228, DOI: 10.3390/antiox10020228.
78 M. Liang, Z. Wang, H. Li, L. Cai, J. Pan, H. He, Q. Wu, Y. Tang, J. Ma and L. Yang, *Food Chem. Toxicol.*, 2018, **115**, 315–328, DOI: 10.1016/j.fct.2018.03.029.
79 K. Stefanowska, M. Woźniak, R. Dobrucka and I. Ratajczak, *Materials*, 2023, **16**(4), 1579, DOI: 10.3390/ma16041579.
80 C. N. Nunes and J.-P. Emond, *Proc. Fla. State Hortic. Soc.*, 2007, **120**, 235–245.
81 J. Liu, S. Liu, X. Zhang, J. Kan and C. Jin, *Postharvest Biol. Technol.*, 2019, **147**, 39–47, DOI: 10.1016/j.postharvbio.2018.09.004.
82 L. K. Kurabetta, S. P. Masti, M. P. Eelager, M. N. Gunaki, S. Madihalli, A. A. Hunashyal, R. B. Chougale, P. Kumar, S. K and A. J. Kadapure, *Int. J. Biol. Macromol.*, 2023, **227**, 127552, DOI: 10.1016/j.ijbiomac.2023.127552.
83 Y. Zhao, R. Tian, Q. Zhang, L. Jiang, J. Wang, Y. Zhang and X. Sui, *Carbohydr. Polym.*, 2024, **332**, 121903, DOI: 10.1016/j.carbpol.2024.121903.
84 J. Liu, Y. Dong, X. Zheng, Y. Pei and K. Tang, *Food Chem.*, 2024, **438**, 138009, DOI: 10.1016/j.foodchem.2023.138009.
85 K. Sari, F. Y. Affandi, B. Nugraha, M. Anwar, A. Pamungkas, A. S. Praharasti, I. M. Janah, H. Hernawan and N. A. Bahmid, *Int. J. Biol. Macromol.*, 2025, **322**, 146948, DOI: 10.1016/j.ijbiomac.2025.146948.
86 Z. H. Zhang, Z. Han, X. A. Zeng, X. Y. Xiong and Y. J. Liu, *Int. J. Biol. Macromol.*, 2015, **81**, 638–643, DOI: 10.1016/j.ijbiomac.2015.08.042.
87 S. Dodange and H. Shekarchizadeh, *Ind. Crops Prod.*, 2025, **225**, 122168, DOI: 10.1016/j.indcrop.2025.122168.
88 J. Li, Y. Hou, S. Song and H. Chen, *Int. J. Biol. Macromol.*, 2026, **336**, 149320, DOI: 10.1016/j.ijbiomac.2025.149320.
89 J. Zhu, Y. Tang, L. Lu, X. Qiu and L. Pan, *React. Funct. Polym.*, 2024, **197**, 105861, DOI: 10.1016/j.reactfunctpolym.2024.105861.
90 W. Lai, L. Wang, Y. Pang, M. Xin, M. Li, L. Shi and Y. Mao, *Food Chem.*, 2024, **455**, 139908, DOI: 10.1016/j.foodchem.2024.139908.
91 L. K. Kurabetta, S. P. Masti, M. P. Eelager, M. N. Gunaki, S. Madihalli, A. A. Hunashyal, R. B. Chougale, P. K. S. Kumar and A. J. Kadapure, *Int. J. Biol. Macromol.*, 2023, **227**, 127552, DOI: 10.1016/j.ijbiomac.2023.127552.
92 H. Yu, Y. Ge, H. Ding, Y. Yan and L. Wang, *Int. J. Biol. Macromol.*, 2023, **253 Pt 2**, 126726, DOI: 10.1016/j.ijbiomac.2023.126726.
93 H. Wang, L. Wang, S. Jia, Q. Feng, L. Guo, S. Zhang and Y. Yu, *Int. J. Biol. Macromol.*, 2025, **309**, 142972, DOI: 10.1016/j.ijbiomac.2025.142972.